Proceedings of the 6^{th} International Conference on Fluid Flow and Thermal Science (ICFFTS 2025)

Barcelona, Spain - October 29 - 31, 2025

Paper No. 124

DOI: 10.11159/icffts25.124

Implementation of Porous Media and Mass Sink Boundary Conditions for Stable Wave Generation in CFD

Miguel Gil¹, Javier Leon¹, Juan Pablo Fuertes¹, Alexia Torres¹

¹Public University of Navarra Av. Cataluña S/N, Pamplona, Spain

miguel.gil@unavarra.es; javier.leon@unavarra.es; juanpablo.fuertes@unavarra.es; alexia.torres@unavarra.es

Abstract - This work presents a numerical strategy to reduce computational cost in the simulation of second-order Stokes waves using Simulia XFlow. Due to the limitations of Active Wave Absorption methods in XFlow, passive techniques were explored. A porous media region and a mass sink were implemented to mitigate wave reflections at the outlet boundary, allowing for an increase in time step without significantly compromising accuracy. A parametric study was performed by varying the Courant number and the vertical position of the mass sink. Results demonstrate that, although minimal loss in accuracy is observed compared to the base case, the proposed setup substantially reduces computational time. Specifically, by implementing this technique, computational cost can be reduced by 94.5% by increasing error only a 15%, making it a promising setup for future large-scale offshore simulations.

Keywords: 4 - 8 keywords

1. Introduction

The usage of CFD software for the hydrodynamic simulation of floating offshore platforms in wind industry is an increasing resource among researchers in this area. This method allows predicting the behaviour of wind turbines in extreme wind and wave conditions, with the computational cost being one of the main drawbacks of this technique. The computational cost of CFD simulations is directly related to the number of elements, mesh size, and time step size, all of which can directly affect the accuracy of the simulation. Simulia XFlow is a CFD software based on the Lattice Boltzmann method that integrates tools for the stable generation of second-order of Stokes waves, among others. However, its high computational cost means that its use is limited, as it requires a short step time to work correctly. The increase in time step reduces the computational cost but causes wave reflection effects at the outlet boundary condition that completely distort the wave simulation as the simulation time progresses. There are different tools to reduce reflection effects, among which Active Wave Absorption [AWA] [1] methods stand out, which act on the wave generation condition from flow measurements. This technique cannot be implemented in XFlow due to programming limitations. On the other hand, Passive Wave Absorption [PWA] methods can be used, such as the introduction of relaxation zones [2], dissipative beaches [3] and buffer zones such as sponge layers [4]. The use of dissipative beaches implies an excessive increase in the study channel, so it is usually useful in experimental tests. On the other hand, the use of sponges reports an increase in the free surface level of the channel, so it is usually necessary to introduce mass sinks to correct this effect [5]. The objective of this study is focused on the simulation of stable wave conditions for the simulation of full-scale floating wind turbines with a reduced computational cost. To this end, the implementation of sponge-type boundary conditions to reduce the reflection effect resulting from the increase in time step, and the savings in computational cost that this entails are analyzed. In addition, a mass sink is introduced to limit mass gain inside the channel, and its position is optimized for different passage times, keeping the element size constant.

2. Simulation setup

This study focuses on the simulation of full-scale second-order Stokes waves of period T=10 s, wave amplitude A=3 m and wavelength λ =156 m, used in numerous simulations of full-scale floating wind turbine platforms. [6]. The objective is the analysis of boundary conditions and reduction of reflection effects, for which simulations are performed in 2 dimensions, and whose results will be extrapolated to simulations in 3 dimensions in more advanced phases. This allows a deeper study due to the limited computational cost of this type of simulations.

2.1. Computational domain and boundary conditions

The computational domain used (Fig. 1) has a length of 624 m, corresponding to 4 wavelengths, and 200 m depth, respecting a mean free surface height of 182.4 m, which corresponds to the wave depth h. With respect to the base model, implementing porous media implies increasing the channel size, which also results in an increase in the number of elements and therefore in the simulation time. However, it allows to increase the time step sufficiently to counteract this effect.

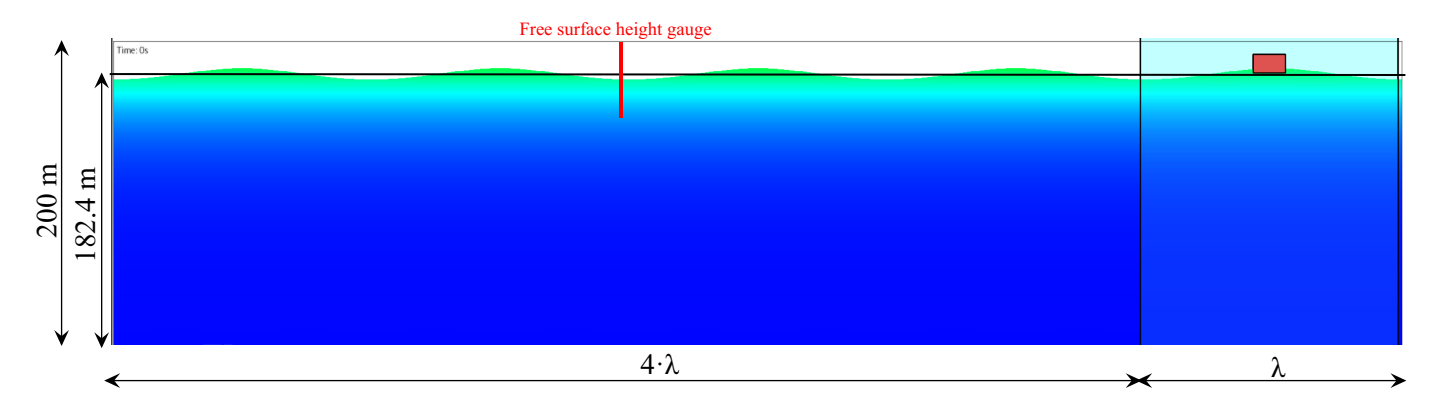


Fig. 1: Computational domain setup

In the downstream region of the channel a porous material is included to generate a pressure jump in the fluid with a length of $1 \cdot \lambda$, which helps to dissipate kinetic energy of the waves and to reduce reflection effects. The generated pressure jump is defined by Eq (1), where ρ is the fluid density, μ the viscosity and v the fluid velocity. The Ergun coefficient C_E is set to 0.2, and the permeability K is set according to Eq (2), where x_0 is the right-hand coordinate of the porous material, x_s is the length of the porous layer and x the global coordinate of the space. For this particular case α =5 and n=2 have been set, showing good results in previous cases for this mesh.

$$\Delta P = \frac{\mu}{K} \cdot \nu + \frac{C_E \mu}{\sqrt{K}} \cdot \nu^2 \tag{1}$$

$$K = \alpha \cdot \frac{exp\left[\left(\frac{x_0 - x}{x_s}\right)^n\right] - 1}{exp(1) - 1}$$
(2)

A box with convective outlet boundary condition is introduced inside the porous material at a height H, which acts as a mass sink eliminating any fluid element that comes in contact with it. Its bottom surface is taken as reference, and H=0 m is set when this surface coincides with the mean water depth.

2.2. Grid conditions

A 3-level grid is implemented in the simulation, employing a coarse element size of 1.2 m and a 0.3 m size element in the free surface, according to Lattice Boltzmann meshing method shown in Fig. 2. The selection of this mesh is because it is meant to be implemented in the simulation of full-scale floating platform with 0.15 m element size in the vicinity of the geometry.

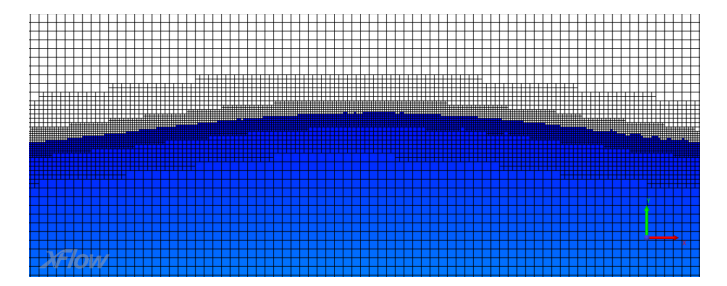


Fig. 2: Grid sample.

3. Loadcase

The same simulation is performed using different time steps, in order to analyse the effect in the precision of the results and the computational cost. Time step (t_s) is defined by Courant number C, following Eq. 3, where v_{ref} is the reference velocity and considered as the celerity (λ/T) and Δx is the wake element size. 5 different Courant number are studied and are named as C_1 =1.3, C_2 =0.975, C_3 =0.812, C_4 =0.65 and C_5 =0.325,

Also, the position of the mass sink is calibrated in order to find its optimal position and the minor error of the simulation for each Courant. The selected positions are $H_1=2.4$ m, $H_2=1.8$ m, $H_3=1.2$ m, $H_4=0.6$ m, $H_5=0$ m and $H_6=-0.6$ m.

In total, 35 simulations are performed, named following the nomenclature C_xH_y.

$$C = \frac{v_{ref} \cdot t_s}{\Delta x} \tag{3}$$

Four additional simulations are performed varying the Courant and using the base tool implemented in XFlow, using the same mesh and domain dimensions but without introducing porous regions and mass sinks. These simulations set the reference of the base computational cost, and of the accuracy in the results obtainable for the selected mesh. The studied courants are C_{t1} =0. 325, C_{t2} =0.1625, C_{t3} =0.08125 and C_{t3} =0.0406.

4. Results

Wave height is monitored throughout the 500-second simulation using a free-surface height gauge located 312 m from the entrance of the channel, where floating elements are intended to be introduced in subsequent simulations.

4.1. Mean Square Error

The results of the last 10 wave cycles are compared against the theoretical wave height, and the mean square error (MSE) is calculated. This measure is affected by variations in period and wave height, so it provides a more complete overview than a reflection coefficient analysis.

Fig. 3 shows the mean square error obtained for each simulation with porous medium and mass sink, painting on the horizontal axis the height H for each simulated Courant. First, it should be noted that the increase in Courant is directly related to the increase in MSE, except for those C_5H_y , finding a minimum at C_4H_y . This effect is observed in Fig. 4, where the MSE is observed for each Courant and for the optimal position of H. In addition, the MSE obtained for the reference simulations where neither porous materials nor mass sink are introduced is shown.

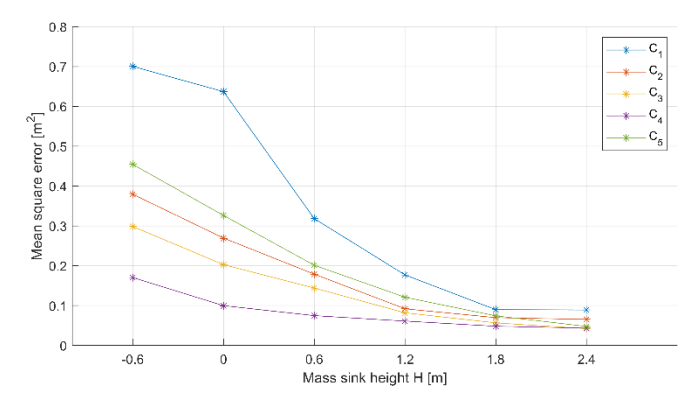


Fig. 3: MSE as a function of the mass sink height for each Courant number.

Fig. 4 shows that the increase of the Courant in the base models implies a drastic increase in the MSE, especially from C_{t2} onwards, which forces the use of short time steps to guarantee the accuracy of the simulation, and justifies the need to use porous media and mass sinks if the simulation time is to be reduced.

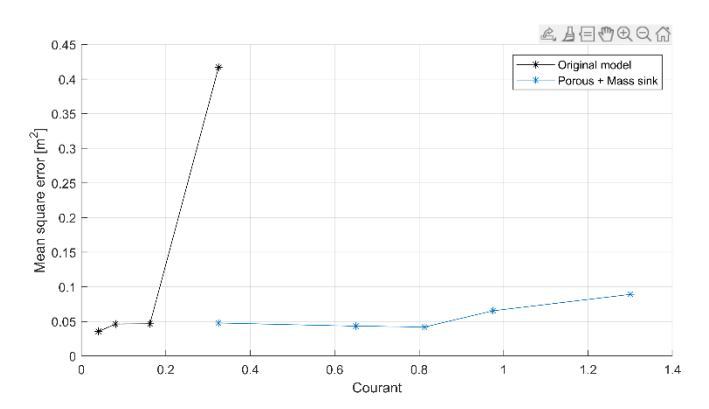


Fig. 4: MSE for optimized H, as a function of the Courant, and MSE for reference simulations.

For the base models, a minimum MSE of 0.035 m² is obtained, while for the porous models the minimum MSE is 0.043 m². Based on this measure alone, the use of these techniques cannot be justified, but it is necessary to review the simulation time for each of them.

4.2. Simulation time

This increase in Courant has an impact on the computational cost of the simulations. Fig. 5 shows the simulation time of the last 10 cycles as a function of the Courant. The position of the convective box hardly affects the computational cost, so the average simulation time is shown sorted by C_xH blocks. For the case C=0.325, a small increase of the computational cost is observed for the models with porous medium, consequence of the dimensions of the domain with respect to the reference model.

In general, it is observed that the reduction of the step time leads to an exponential increase in the simulation time, independently of the boundary conditions used.

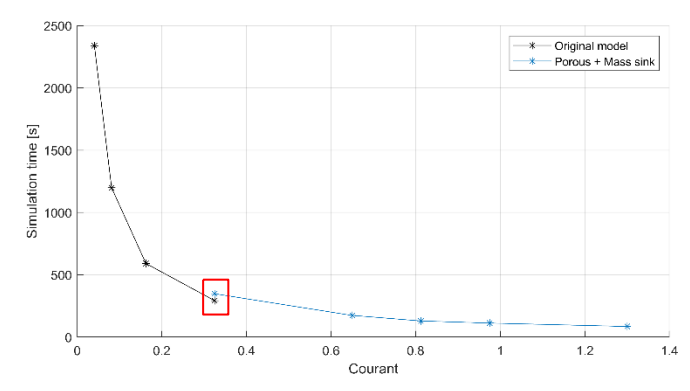


Fig. 5: Simulation time VS Courant

4.3. Simulation time vs MSE comparison

Both aspects analyzed in previous sections are key in simulation, so the following analysis is made to consider both parameters and analyze the improvement of the proposed boundary conditions.

First of all, a non-dimensionalization of MSE is made by dividing it by the theoretical wave height (2·A) according to Eq (4). Also, simulation time is non-dimensionalized by the theoretical wave period according to Eq (5).

$$MSE_{adim} = \frac{MSE}{(2 \cdot A)^2}$$

$$t_{adim} = \frac{t_{sim}}{T}$$
(5)

$$t_{adim} = \frac{t_{sim}}{T} \tag{5}$$

Reducing both parameters is important, so the simulation near to the graph origin in Fig. 6 is the one that shows better relation between parameters, so the module is computed. However, simulation time values are predominant over error, so first the variables are expressed in unitary form, dividing both by the maximum value obtained in all simulations. Fig. 6 shows the MSE_{adim} with respect to t_{adim} expressed in unitary form.

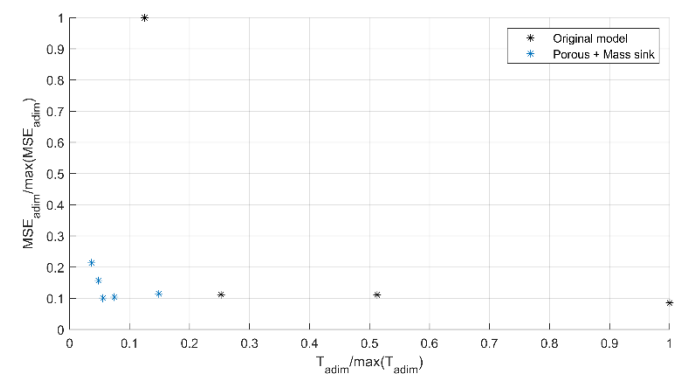


Fig. 6: Dimensionless MSE VS dimensionless simulation time, in unitary form.

According to Fig. 6, all simulation employing porous media are closer to the origin, showing better relation between error and simulation time, and C₃H₁ being the closest. This model is compared to theoretical simulation C_{t3}, which has 15% less error, but requires 94.5% more simulation time.

Finally, Fig. 7 shows the wave elevation for the simulations that shows less error for both types of boundary conditions and compared to theoretical one. This figure shows that porous media simulations underpredict wave amplitude, but shows a better fit to theoretical, compared to reference one that overpredict it.

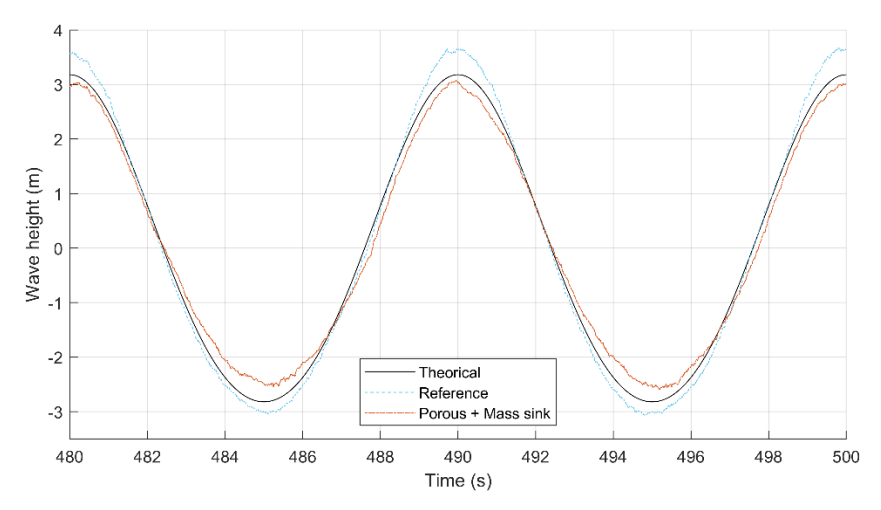


Fig. 7: Surface elevation over last 2 wave periods.

5. Conclusions

This study evaluated passive boundary conditions to mitigate wave reflections in CFD simulations using Simulia XFlow, particularly when increasing the Courant number to reduce computational time. The implementation of a porous medium at the outlet and a convective mass sink proved effective in maintaining wave stability. The following conclusions are obtained:

- Increasing the Courant number generally increases the mean square error (MSE), but the use of porous media and mass sinks mitigates this effect.
- The simulation setup C₃H₁ provides the best trade-off, reducing simulation time by over 95% with only a 15% increase in MSE compared to the theoretical reference case.
- Simulations without boundary treatment showed significant loss in accuracy at Courant numbers above 0.1625, justifying the need for additional wave damping mechanisms.

The methodology enables more efficient simulations for large-scale offshore platforms and could be extended to 3D scenarios or coupled CFD-structure interaction studies in future work.

References

- [1] T. Vyzikas, D. Stagonas, E. Buldakov y D. Greaves, «The evolution of free and bound waves during dispersive focusing in a numerical and physical flume,» *Coastal Engineering*, vol. 132, pp. 95-109, 2018.
- [2] D. Fuhrman, M. Per y B. Harry, «Numerical simulation of lowest-order short-crested wave instabilities,» *Journal of Fluid Mechanics*, vol. 563, pp. 415-441, 2006.
- [3] A. Magee, V. Nelko, K. Y. Lim y L. W. Chew, «Benchmarking Experiments for Wave Absorption Modeling,» de *Honoring Symposium on Marine Hydrodynamics*, St. John's, Newfoundland, 2015.
- [4] J. O. Williams, "Narrow-band analyzer," Ph.D. dissertation, Dept. Elect. Eng., Harvard Univ., Cambridge, MA.
- [5] D. Wang y S. Dong, «A discussion of numerical wave absorption using sponge layer methods,» *Ocean Engineering*, vol. 247, p. 110732, 2022.
- [6] G. Campaña, R. Martín, B. Mendez, P. Benito y J. Azcona, «OF2: coupling OpenFAST and OpenFOAM for high-fidelity aero-hydro-servo-elastic FOWT simulations,» *Wind Energy Science*, vol. 8, no 10, pp. 1497-1611, 2023.